Safety and efficacy of mesenchymal stromal cells mitochondria transplantation as a cell-free therapy for osteoarthritis

Ana Maria Vega-Letter, Cynthia García-Guerrero, Liliana Yantén-Fuentes, Carolina Pradenas, Yeimi Herrera-Luna, Eliana Lara-Barba, Felipe Bustamante-Barrientos, Masyelly Rojas, María Jesús Araya, Nicole Jeraldo, et al.

Journal of Translational Medicine

RESEARCH

Open Access

Safety and efficacy of mesenchymal stromal cells mitochondria transplantation as a cell-free therapy for osteoarthritis

Ana Maria Vega-Letter[9†], Cynthia García-Guerrero[1,2†], Liliana Yantén-Fuentes[1,2], Carolina Pradenas[1,2], Yeimi Herrera-Luna[1,2], Eliana Lara-Barba[1,2], Felipe A. Bustamante-Barrientos[1,2], Masyelly Rojas[2], María Jesús Araya[1,2], Nicole Jeraldo[1,2,8], Constanza Aros[1,2], Francisca Troncoso[1,2], Daniela Poblete[5], Angela Court[1,2,3], Alexander Ortloff[6], Jose Barraza[6], Francesca Velarde[1,2], Carlos Farkas[12], Claudio Carril[10], Noymar Luque-Campos[1,2], Gonzalo Almarza[11], Maximiliano Barahona[15], Jose Matas[1], Lucas Cereceda[1,2], Rocío Lorca[1,2], Jorge Toledo[8], Karina Oyarce[10], Rolando Vernal[5], Andrés Caicedo[13], Andrea del Campo[11], Yessia Hidalgo[1,2,3], Roberto Elizondo-Vega[7], Farida Djouad[4,14], Maroun Khoury[1,2,3*], Fernando E. Figueroa[1,2,3*] and Patricia Luz-Crawford[1,2*]

Abstract

Objective The inflammatory responses from synovial fibroblasts and macrophages and the mitochondrial dysfunction in chondrocytes lead to oxidative stress, disrupt extracellular matrix (ECM) homeostasis, and accelerate the deterioration process of articular cartilage in osteoarthritis (OA). In recent years, it has been proposed that mesenchymal stromal cells (MSC) transfer their functional mitochondria to damaged cells in response to cellular stress, becoming one of the mechanisms underpinning their therapeutic effects. Therefore, we hypothesize that a novel cell-free treatment for OA could involve direct mitochondria transplantation, restoring both cellular and mitochondrial homeostasis.

Methods Mitochondria were isolated from Umbilical Cord (UC)-MSC (Mito-MSC) and characterized based on their morphology, phenotype, functions, and their ability to be internalized by different articular cells. Furthermore, the transcriptional changes following mitochondrial uptake by chondrocytes were evaluated using an Affymetrix analysis, Lastly, the dose dependence therapeutic efficacy, biodistribution and immunogenicity of Mito-MSC were assessed in vivo, through an intra-articular injection in male C57BL6 mice in a collagenase-induced OA (CIOA) model.

Results Our findings demonstrate the functional integrity of Mito-MSC and their ability to be efficiently transferred into chondrocytes, synovial macrophages, and synovial fibroblasts. Moreover, the transcriptomic analysis showed

†Ana Maria Vega-Letter and Cynthia García have contribute equally to this work.

*Correspondence:
Maroun Khoury
mkhoury@uandes.cl
Fernando E. Figueroa
ffigueroa@uandes.cl
Patricia Luz-Crawford
pluz@uandes.cl
Full list of author information is available at the end of the article

the upregulation of genes involved in stress such as DNA reparative machinery and inflammatory antiviral responses. Finally, Mito-MSC transplantation yielded significant reductions in joint mineralization, a hallmark of OA progression, as well as improvements in OA-related histological signs, with the lower dose exhibiting better therapeutic efficacy. Furthermore, Mito-MSC was detected within the knee joint for up to 24 h post-injection without eliciting an inflammatory response in CIOA mice.

Conclusion Collectively, our results reveal that mitochondria derived from MSC are transferred to key articular cells and are retained in the joint without generating an inflammatory immune response mitigating articular cartilage degradation in OA, probably through a restorative effect triggered by the stress antiviral response within OA chondrocytes.

Keywords Mitochondria transplantation, Mesenchymal stromal cells, Osteoarthritis, Murine OA model, Biodistribution, Immuno-safety

Introduction

OA is a worldwide degenerative disease, with only palliative treatments. OA progression involves synovial inflammation (driven by synovial macrophages and fibroblasts) and mechanical failures negatively affecting chondrocytes, the main components of hyaline cartilage [1–3]. This leads to ROS production with concomitant mitochondrial DNA damage followed by mitochondrial dysfunction [4]. Mitochondrial transplantation has emerged in the last year as a thriving approach to treat several diseases associated with mitochondrial dysfunction, including osteoarthritis (OA) [5–11]. In a Wistar rat model of osteoarthritis (OA), mitochondria derived from the L6 rat cell line (mito-L6) and muscle derived from OA patients (mito-muscle OA) have shown a beneficial effect on OA progression. This is evidenced by improved histological scores and enhanced mitochondrial function in chondrocytes from OA rats, suggesting a chondroprotective role for exogenous mitochondrial transplantation in OA [12]. However, to translate this effect into therapeutic use, it is necessary to utilize cells that can be consistently obtained, are well-studied (with known characteristics), and have clinical potential. Mesenchymal stromal cells (MSC) meet these criteria, as they have been extensively used in clinical studies [13–15], demonstrating anti-inflammatory properties and the ability to mitigate cartilage degeneration in preclinical assays [13, 16, 17]. Furthermore, in vitro, they have shown the capacity to transfer their mitochondria to human chondrocytes, increasing the gene expression of aggrecan, a critical proteoglycan of hyaline cartilage and inhibiting chondrocyte apoptosis [18, 19]. Consistent with this study, a bovine cartilage explant injury model demonstrated that MSCs can transfer their mitochondria in situ into bovine chondrocytes [20]. However, the dose-dependent efficacy of mitochondria, biodistribution, clearance and potential immunogenicity effect has not been addressed. Therefore, in the present study, we sought to: (1) Assess the mitochondrial transfer from human umbilical cord-derived MSCs (UC-MSCs) to primary OA cells, including chondrocytes, synovial fibroblasts, and synovial macrophages, (2) Evaluate the potential transcriptomic changes of mitochondria transfer into human chondrocytes that drive their therapeutic effect and to (3) Determine the dose-dependent effect of mitochondria, including their biodistribution and immunogenicity. This study reveals that MSC-derived mitochondria are (i) transferred into the main target cells of osteoarthritis in vitro, (ii) inducing transcriptomic changes in chondrocytes associated with DNA reparative machinery and inflammatory antiviral responses and (iii) are retained in the mouse knee joint for more than 24 h after their IA injection with a significant improvement in function, without exerting adverse immunogenic effects.

Materials and methods

Bioethics

All methods were carried out following guidelines and regulations for using animals. All the procedures presented in this work were approved by the Ethics Committee of Universidad de Los Andes (Folio CEC No. 202033) and by the Ethics Committee of Universidad de Chile (Approval Certificated No. 12). All recruited patients signed informed consent forms before donating tissue.

Animals

C57BL6 male littermates mice were housed together in individually ventilated cages with three to four mice per cage. All mice were maintained on a regular diurnal lighting cycle (12:12 light: dark) with ad libitum access to food and water. Mice were housed under broken barrier-specific pathogen-free conditions in the animal facility of Cells for Cells, according to the guidelines of the Cells for Cells Guide for the Care and Use of Laboratory Animals.

Human OA samples

Chondrocytes, synovial macrophages, and synovial fibroblasts were isolated from female and male donors, aged

40–90, diagnosed with knee or hip OA presenting with functional limitation, who underwent total hip or knee replacement at either Clínica Universidad de Los Andes or at Hospital Clínico Universidad de Chile (HCUCH). Specific protocols for the isolation of chondrocytes, synovial macrophages and synovial fibroblasts are in Supplementary material. OA samples were obtained from both the knee and hip to provide a broader understanding of the disease and assess the treatment effects on OA overall. Furthermore, the use of both samples was influenced by the availability of clinical samples, ensuring an adequate sample size for in vitro experiments.

Mitochondria isolation and in vitro transfer to chondrocytes, synovial macrophages, and fibroblasts

Mitochondria derived from Human UC-MSCs were isolated from the umbilical cords of healthy, voluntary pregnant women, regardless of the sex of the baby were isolated from previously MitoTracker™ deep red (Invitrogen™, USA) labeled cells using the Mitochondria Isolation Kit (ThermoFisher Scientific, USA), following manufacturer's instructions. After isolation, mitochondria were resuspended in media and were maintained on ice until in vitro transfer following the "Mitoception" protocol as previously described [21]. For that purpose, cells were previously labeled with an MT specific fluorescent probe, MitoTracker Green, following the manufacturer's instructions. Cells were seeded on a cover slide previously coated with poly-lysine, and mitoception was performed using the amount of UC-MSC:Mito corresponding to UC-MSC: Acceptor cell ratios of 1:1 for chondrocytes and synovial fibroblasts, and 1:10 for synovial macrophages, which was selected according to the minimal dose necessary to observed an efficient mitochondrial transfer. Twenty-four hours after artificial mitochondrial transfer, acceptor cells were obtained, and fixed for mitochondrial transfer evaluation by confocal microscopy with a Leica TCS SP8 confocal laser system. The percentage of mitochondria transfer was determined by FACS using the BD FACSCanto™ II (BD Pharmingen).

Mitochondria functional and phenotypic characterization

Mitochondria were isolated from UC-MSC using the Cell Mitochondria Isolation Kit (ThermoFisher Scientific, USA) following manufacturing instructions. Mitochondria characterization and function were assessed by Transmission Electron Microscopy (TEM) to evaluate their structure, Flow cytometry to determine the expression of specific mitochondrial markers, oxygen consumption measurement and ATP content quantification. Specific protocols for their functional and phenotypic characterization are in the Supplementary material.

Collagenase-induced osteoarthritis model

Collagenase-induced OA (CIOA) model was carried out as previously described [5]. Briefly, 1U type VII collagenase in 5 µL saline was administered via intra-articular injection (IA) in the knee joint of C57BL/6 mice (10 weeks old) at days 0 and 2 for OA induction. Groups of 10 mice received MSC IA (2×10^5-High dose and 0.5 cells $\times10^5$-low dose/5 µL saline), on days 7 and 14. At day 42, mice were euthanized, and paws were carefully dissected to remove any remaining tissue prior to microCT scanning and then fixed in 4% formaldehyde followed by a demineralization protocol with 5% formic acid for 3 weeks for histological analysis.

MicroCT analysis

The samples were analyzed using X-ray microtomography using a Micro-CT SkyScan 1278 (Bruker, Belgium, 0.5 mm aluminum filter, 20–65 kV, 500µA, resolution of 50 µm, 0.5° rotation angle) provided by the Universidad de Chile, using characteristics defined by the equipment operator. 3D Scans were reconstructed using NRecon software (Bruker, Belgium). Misalignment compensation, ring artifacts, and beam-hardening were configured to obtain a correct reconstruction of each paw. Bone mineral density, BS/BV and thickness were quantified in the 4 knee zones: lateral subchondral, medial subchondral, lateral femur, and medial femur of each paw (CTAn software, Bruker, Belgium).

Histological analysis

Hind paws were decalcified after a 3-week incubation within a formic acid 5% solution and then embedded in paraffin. Tibias were sectioned frontally as previously described [16] and stained with safranin O fast green. Quantification of the degradation of cartilage was performed using the modified Pritzker OARSI score as described [22].

Biodistribution analysis in CIOA murine model

After 80% of confluence, UC-MSC were trypsinized and stained with Mitoview720 (Biotium, USA) at 10 mM for 20 min at 37 °C. Mitochondria derived from UC-MSC were obtained using the mitochondria isolation kit for mammalian cells (Invitrogen, USA). Mice were intraarticularly injected with Mitoview stained-mitochondria derived from 200.000UC-MSC/5 µL into the right knee joint while the contralateral knee was used as a sodium chloride sham control. Detection of fluorescent imaging of OA mice was evaluated at 0, 1 h, 24 h, 48 h and 72 h in an Odyssey CLx Imager (LI-COR) with the Mouse Pad accessory to maintain the body temperature of anesthetized mice at 37 °C. At 72 h, organs were obtained and

observed in the Odyssey CLx Imager (LI-COR) to detect potential mitochondria leakage into other organs. In parallel, we performed a human mitochondrial DNA quantification. For that purpose, at day 7 post OA induction, mice were injected intraarticularly with mitochondria derived from MSC and euthanized at 0, 1 h, 24 h, 48 h and 72 h post-mitochondria injection. Knees, draining and popliteal lymph nodes were collected, and total DNA was extracted using the Dneasy Blood &Tissue total DNA isolation kit (Qiagen, USA), following manufacturing instructions. An endogenous control was also amplified to identify the murine mitochondrial genome. Primers´ sequences were as follows: murine mitochondrial genome mouse, forward 5′-CTAGAAACCCCG AAACCA AA-3′, reverse 5′-CTAGAAACCCCGAAA CCAAA3′; human mitochondrial genome, forward F3 5′-CACTTTCCACACAGACATCA-3′, reverse 5′-TGG TTAGGCTGGTGTTAG GG-3′. The thermal profile for mtDNA detection was: pre-incubation at 95 °C for 5 min (one cycle); denaturation at 95 °C for 10 s; annealing and extension at 60 °C for 30 s (denaturation and extension steps for 40 cycles); melting at 95 °C for 5 s, 60 °C for 1 min, 95 °C for 15 s, and, the last step, cooling at 40 °C for 30 s. When specific melting curves for the human mitochondrial genome were identified the sample was considered positive for the presence of human mitochondrial DNA.

Immunogenicity evaluation in CIOA murine model

Mice were euthanized on day 14 of OA induction and the draining popliteal lymph nodes were recovered for disaggregation. Extracted cells were passed through a 40-µm filter (cell strainer; BD Falcon) and centrifuged at 1680 rpm for 6 min. Then, cells were cultured with PMA (50 ng/mL) (Sigma) and Ionomycin (1 µg/mL) (Sigma-Aldrich) in the presence of 10 µg/mL brefeldin A (Biolegend, USA). After 4 h, standard intracellular staining was carried out to identify the CD4+, IFN-γ+, IL17+, CD25+ high, and Foxp3+ cells. For this, cells were fixed and permeabilized using the FOXP3 transcription factor staining buffer (Invitrogen™, USA), according to the manufacturer's instructions. The acquisition was performed with a BD FACSCanto™ II using the FlowJo software (version 10.0.7) measured by flow cytometry.

Human RNA isolation

Four samples of chondrocytes derived from OA patients (Chondro-OA) were cultured and incubated with mitochondria using the protocol described by Caicedo et al. [21]. Then, RNA was obtained using the miRNA isolation kit (Qiagen, France) from Chondro-OA to evaluate the potential RNA differences upon artificial mitochondria transfer. The sequencing was performed with a human Affymetrix® ZebGene 1-0-ST Array (Life Technologies, France), in the transcriptomic platform in the IRMB Institute at Montpellier, France.

Data preparation and differential expression analysis

The raw Affymetrix data were processed using R software (version 4.1.2). Gene expression data were loaded into R and formatted as a data frame using the **dplyr** library (version 1.1.2). The **limma** package (version 3.50.0) was used to analyze differential expressions between different conditions. Genes were considered statistically significant if the adjusted p-value (adj.P.Val) was <0.05.

A design matrix incorporating both subject effects and treatment conditions was constructed to adjust for these variables in the analysis. Contrast matrices were created to directly compare the relevant groups, and the empirical Bayes method was applied to moderate the standard errors of the estimated log-fold changes. The pseudocode is as follows:

$$\boldsymbol{DefineTreatmentandDesignfortheMatrix}$$

$$Treatment < -factor(rep(c(\mathrm{OAC}, \mathrm{mito}), each = 4))$$
$$design < -model.matrix(\sim Subject + Treatment)$$

$$\boldsymbol{Fitlinearmodelstoeachgeneusingthedesignmatrix}$$
$$fit < -lmFit(selected_{data}, design)$$
$$contrast.matrix < -makeContrasts(OACvsMito = TreatmentOAC, levels = design)$$
$$\boldsymbol{Re-fitthemodelsusingthecontrastmatrixand\ ApplyEmpircalBayes}$$
$$fit2 < -contrasts.fit(fit, contrast.matrix)$$
$$fit2 < -eBayes(fit2)$$

Differentially expressed genes were identified based on the following thresholds: adj.P.Val < 0.05 and $|\mathrm{logFC}| \geq 1$. Volcano plots were generated using the EnhancedVolcano package (version 1.10.0) in R, highlighting genes of interest based on log-fold change and adjusted p-value thresholds.

Gene ontology, pathway and network analyses

Significant gene expression changes were visualized using the **Seaborn** package (version 0.12.2) in Python, which enabled the creation of a clustered heatmap to display gene expression patterns across conditions. Expression values were normalized using Z-scores to facilitate clustering, and the resulting heatmap illustrated key expression trends for the differentially expressed genes (DEGs). Pathway and gene ontology (GO) term enrichment analyses were conducted using the **gProfiler** tool through its R API (version 1.0.0). This analysis aimed to identify the biological processes and pathways significantly associated

with the DEGs, providing insights into the functional implications of the observed transcriptional changes. The analysis covered GO terms for Biological Processes (GO), Transcription Factor (TF) enrichment, and Reactome Pathways (REAC). Additionally, KEGG pathways were explored for insights into metabolic and signaling pathways. Results were visualized as bar plots using the **Matplotlib** (version 3.7.1) and **Seaborn** libraries to highlight the most enriched terms and pathways.

To visualize gene networks, we utilized the **STRING** online server (https://string-db.org/) (version 11.5) to construct protein–protein interaction (PPI) networks. The STRING database provides both experimental and computationally predicted interactions between proteins. We inputted the list of DEGs into STRING to query the database and identify high-confidence interactions, applying a confidence score threshold of 0.7. The resulting interaction network was analyzed to identify central nodes (key proteins) that could represent crucial regulatory factors in the biological processes being studied.

Statistical analysis

For the preclinical assay, results were expressed as the mean ± SD. For the in vivo studies (CIOA) 8 to 10 animals were used for each experimental or control group, and experiments were repeated at least two independent times. The p values were generated by parametric analysis using the one-way ANOVA test for multiple comparisons. $p < 0.05$ (*), $p < 0.01$ (**) or $p < 0.001$ (***) were considered statistically significant. All the analyses were performed using the GraphPad Prism TM 6 software (GraphPad Software, San Diego, California, USA).

Results

Mitochondria derived from UC-MSC are functional and are transferred into OA target cells in vitro

Cell-free transfer of mitochondria into pathogenic chondrocytes and synovial macrophages and fibroblasts was evaluated using the mitoception protocol [21] as summarized in Fig. 1a. For that purpose, chondrocytes, synovial macrophages, and synovial fibroblasts were isolated from OA patients and cultured in the presence or absence of freshly isolated mitochondria from UC-MSC previously stained with MitoTracker Deep Red. Before performing the mitoception protocol, mitochondria isolated from UC-MSC were evaluated according to their (i) ATP quantification (Fig. 1b), (ii) respiratory capacity (Fig. 1c), (iii) round-shaped double membrane observed by Transmission Electron Microscopy (TEM) (Fig. 1d) and (iv) expression level and pattern of Tomm20 and mitotracker deep red by flow cytometry (Fig. 1e). Our results showed that mitochondria isolated from UC-MSC were functionally matched since they were isolated from healthy donor cells, present an ATP pool that nearly doubled when the cell count was increased two-fold and showed oxygen consumption (Fig. 1b, c), indicators of efficient respiratory activity. Moreover, they exhibit the round shape double membrane and are positive for Tomm20 and mitotracker™ deep red as demonstrated by TEM (Fig. 1d) and FACS respectively (Fig. 1e). Moreover, mitochondria derived from UC-MSC were successfully acquired by chondrocytes (Fig. 1f, g), synovial macrophages (Fig. 1h, i), and fibroblasts (Fig. 1j, k) as confirmed by the FACS analysis and confocal microscopy images. Overall, these results evidence that MSC-derived mitochondria are effective in targeting the main cell types involved in osteoarthritis.

UC-MSC mitochondria transfer induces transcriptional change in OA chondrocytes

To assess the impact of MSC-derived mitochondrial uptake in cells implicated in osteoarthritis, we conducted a transcriptomic analysis on chondrocytes.

We identified up to 21 upregulated genes and 6 downregulated genes in the human chondrocytes treated with mitochondria from UC-MSC compared to control untreated chondrocytes (Fig. 2a). A heatmap analysis showed clustering between both conditions by a change in the differential gene expression level (Fig. 2b). A search in Gene Ontology (GO) Biological process categories revealed significant terms such as "response to stress", "defense response" and "immune system process", which highlight and activation of immune and stress-related pathways (Fig. 2c, upper-left bar plot). Moreover, we performed pathway enrichment analysis according to Reactome Pathway Annotations and found a significant involvement in "Interferon Signaling" and "Cytokine Signaling in the Immune System", emphasizing a robust immune response (Fig. 2c, low-left bar plot). In addition, we performed a transcription factor (TF) analysis. We found that transcription factors with significant regulatory potential involved in interferon/adaptive immune response are enhanced after treatment with Mito-MSC (Fig. 2c, right bar plot). Finally, we investigated the protein–protein interaction network from STRING analysis (where nodes represent proteins and edges indicate known and predicted interaction among them) (Fig. 2d). Our result showed that key proteins associated to antiviral immune response acting as interaction hubs were accentuated. This result suggests that components of the antiviral immune response seem to display a central role in the response of chondrocytes to mitochondrial treatment. Indeed, we observed a strong network among immune genes induced after mitochondrial treatment, such as USP18, HERC5, USP41, DDX58, and RSAD2, among others. The collective findings indicate that

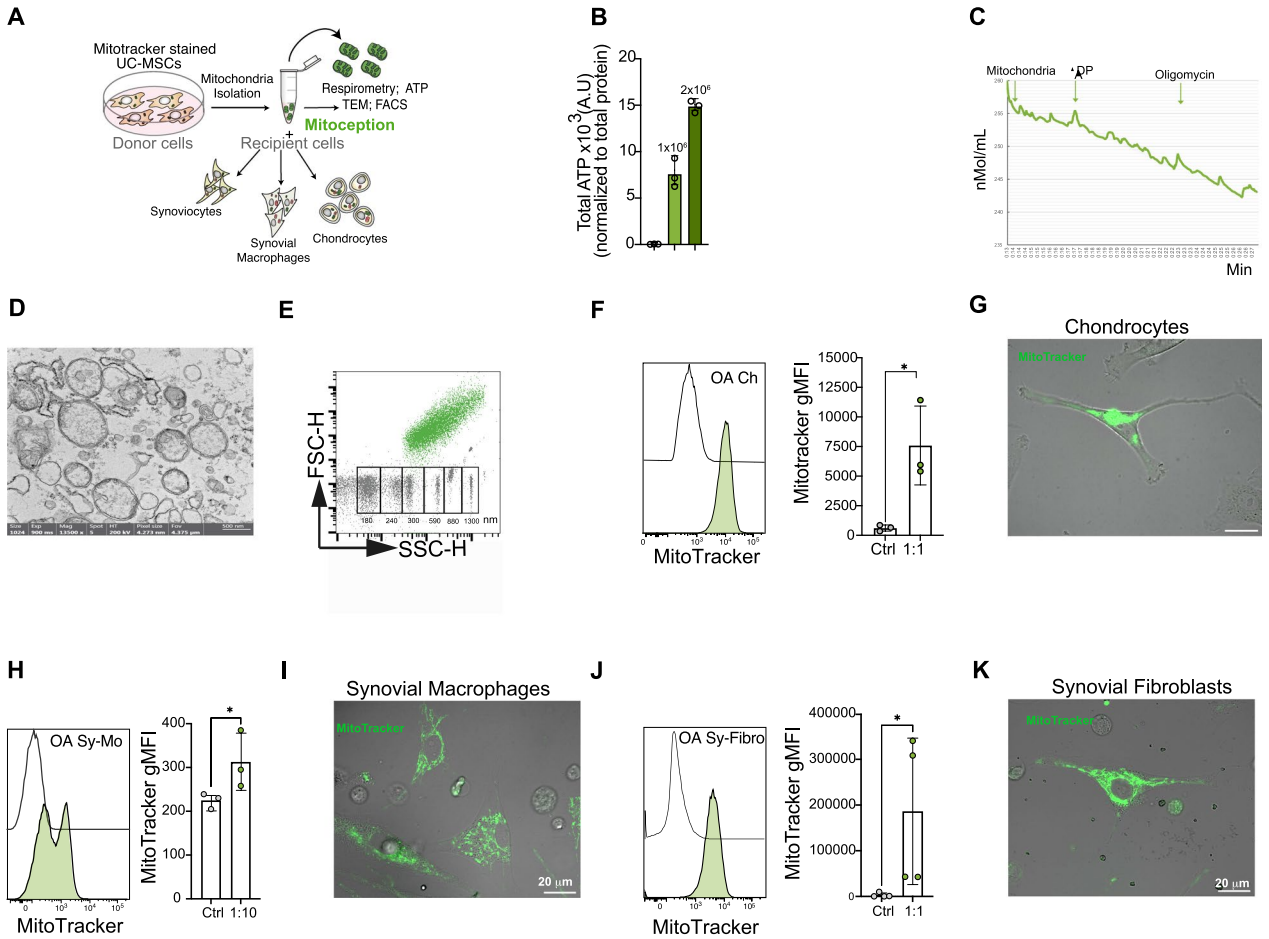

Fig. 1 Artificial transfer of isolated and functional mitochondria derived from UC-MSC to critical OA target cells. **a** Schematic representation of exogenous mitochondria transfers into chondrocytes, synovial macrophages and fibroblasts and the functional characterization of mitochondria derived from UC-MSC. **b** Relative ATP quantification of isolated mitochondria from 3 different UC-MSC donors from 2 different amounts of cells (1 M and 2 M). **c** Oxygen consumption analysis of isolated mitochondria measured with an oxygraph. **d** Electronic microscopy of isolated mitochondria from UC-MSC. **e** FACS dot plot representation of mitochondria stained with Tomm20 and mitotracker™ deep-red. Mitochondria were identified according to the expression of Tomm20 and mitotracker deep-red signal. The size of the mitochondria was evaluated using the apogee beads. **f** Representative FACS histograms of exogenous mitochondria transfer derived from UC-MSC by mitoception into OA-derived chondrocytes (OA-Ch), at a cell ratio of 1:1 (1 OA-Ch:1 Mitochondria derived from UC-MSC) according to the number of UC:MSC. Quantification of the geometric Mean Fluorescence Intensity (gMFI) of the mitotracker signal of mitocepted OA Ch cells from different donors. Confocal microscopy analysis of mitocepted OA Ch. **g** Representative FACS histograms of mitoception of OA-derived synovial macrophages (OA Sy-MO), at a cell ratio of 1:10 (1 OA Sy-Mo:10 Mitochondria derived from UC-MSC), according to the number of UC:MSC. Quantification of the gMFI of mitotracker signals of mitocepted OA Sy-MO cells from different donors. **h** Confocal microscopy analysis of mitocepted OA Sy-MO. **i** Representative FACS histograms of mitoception of OA-derived synovial Fibroblasts (OA Sy-Fibro), at a cell ratio of 1:1 (1 OA Sy-fibro:1 Mitochondria derived from UC-MSC), according to the number of UC:MSC. Quantification of the gMFI of mitotracker signals of mitocepted OA Sy-Fibro cells from different donors. **h** Confocal microscopy analysis of mitocepted OA Sy-fibro. Graphs show mean ± SD and statistical analysis by Mann–Whitney non-parametric test. Each dot represents a different OA patient where at least 3 different donors were evaluated

Mito-MSC transfer induces transcriptional changes in OA chondrocytes, particularly in response to stress and inflammation, two important pathways associated with OA pathology.

Mitochondria transplantation exhibits a pro-regenerative effect in the CIOA murine model independent on the administered dose

To determine whether mitochondrial transplantation exerts a beneficial effect and the dose response, in vivo,

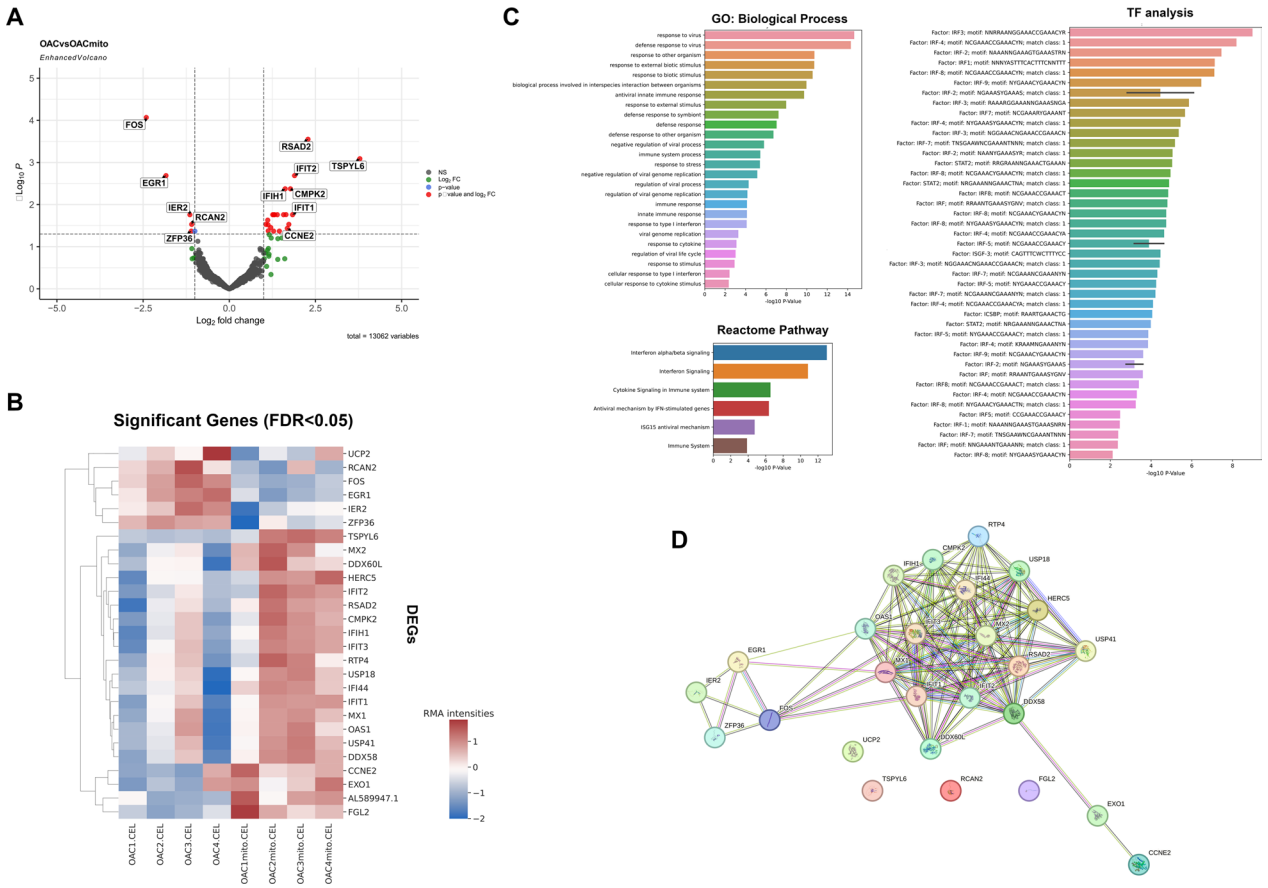

Fig. 2 Gene expression analysis of chondrocytes derived from OA patients with and without UC-MSC derived mitochondria. **a** Volcano Plot illustrating differential gene expression, with log fold change plotted against -log10 adjusted p-values. Genes surpassing significance thresholds are highlighted, demonstrating substantial downregulation and upregulation. **b** Heatmap depicting RMA intensity of significant genes (False Discovery rate < 0.05). Gene names are annotated on the y-axis. Expression levels are represented by a color gradient, with blue indicating lower expression and red indicating higher expression across samples. **c** Bar plots for pathway enrichment analyses. The upper-left plot represents Gene Ontology (GO) Biological Process enrichment. The low-left bar plot displays Reactome Pathway enrichment. The right bar plot represents a Transcription Factor (TF) analysis, which showed TF with significant regulatory potential. **d** Protein–protein interaction network from STRING analysis, where nodes represent proteins and edges indicate known and predicted interactions

we used the collagenase-induced mouse model of OA (CIOA).

To that end, type VII collagenase was injected into the knee joints of mice at days 0 and 2. After 7- and 14-days post OA induction, mitochondria isolated from different amounts of UC-MSC (1×10^6 or $0{,}2\times10^6$ UC-MSC) were injected intraarticularly. At 42 days post-OA induction, histological and histomorphometric studies were

(See figure on next page.)

Fig. 3 Dose Dependance Therapeutic efficacy of mitochondria-derived UC-MSC (Mito-MSC) transplantation in the collagenase-induced osteoarthritis model (CIOA). **a** Schematic representation of the experimental design of the CIOA murine model treated with 2 different doses of mitochondria equivalent to 200.000 UC-MSC (Lower Dose) and the equivalent to 1,000,000 UC-MSC (Higher dose). **b** Schematic representation of the articular joint zones focuses on imaging and histopathological analysis. **c** Representative 3D construction imaging of microCT analysis. Bone mineral density (BMD) and Bone volume Fraction (BS/BV) analysis of CIOA intraarticularly injected or not with Mitochondria derived from UC-MSC at a lower dose (MitoLow) or higher dose (MitoHigh) and control group (sham, contralateral knee injected with vehicle). Average quantification of BMD for **d** Medial Tibia, **e** Lateral Tibia, **f** Lateral femur and **g** Medial femur. Average quantification of BS/BV for **h** Medial Tibia, **i** Lateral Tibia, **j** Lateral femur, and **k** Medial femur. **l** Representative histopathologic images and OA damage score quantification in knee joint sections obtained from the four groups described above for each joint zone. Average quantification of OA histological score according to the Pierce scale for **m** Medial Tibia, **n** Lateral Tibia, **o** Lateral femur, and **p** Medial femur. Graphs represent mean ± SD; $*p \le 0.05$, $**p < 0.01$, $***p < 0.001$. (One-way ANOVA-test) of at least N = 15 animals per experimental group for 2 independent experiments

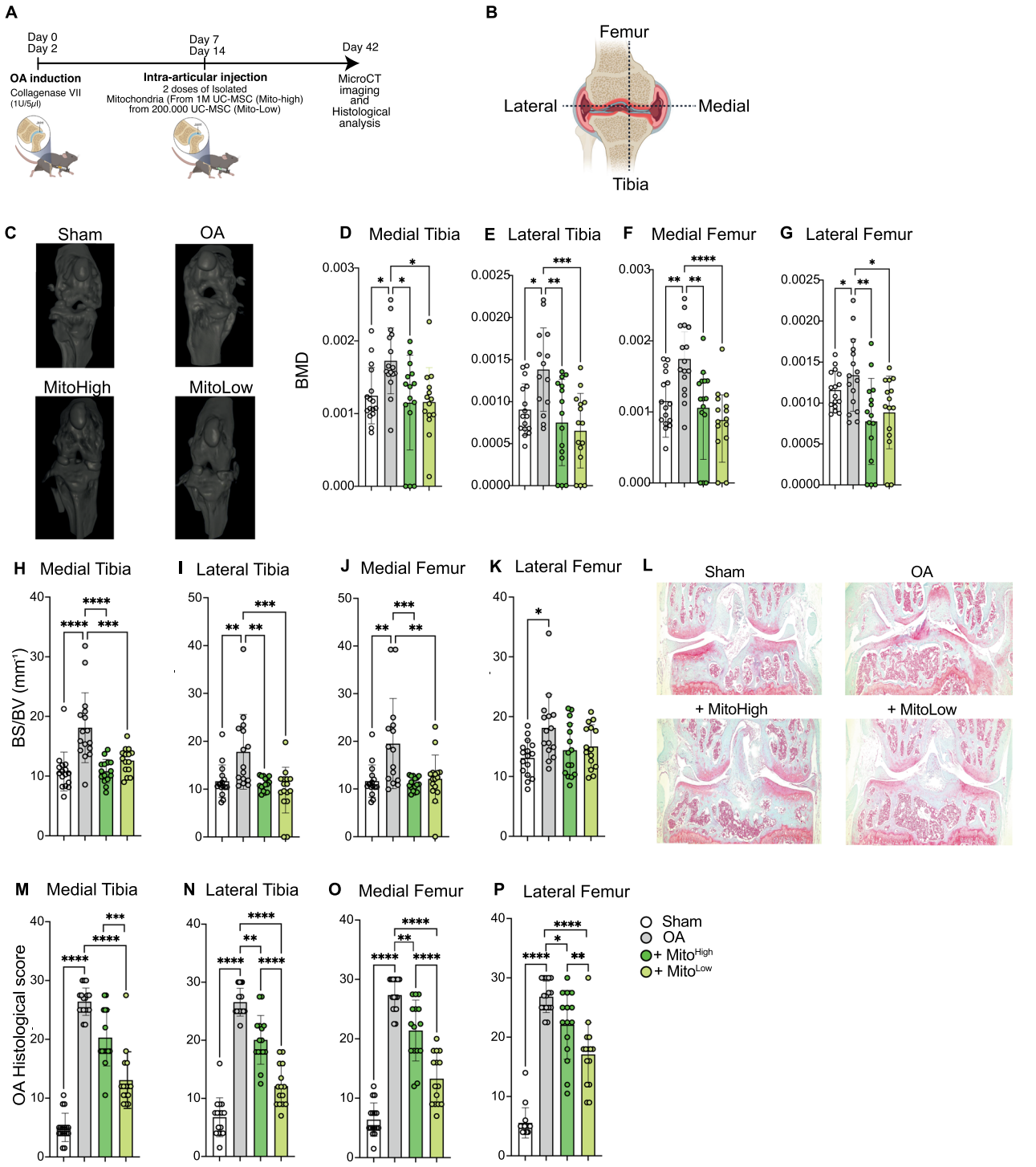

Fig. 3 (See legend on previous page.)

performed to determine the severity of OA (Fig. 3a) in the four zones of the knee (Fig. 3b). Representative 3D images were obtained to evaluate the bone architecture of the joint by micro-computed tomography (µCT) (Fig. 3c). On one hand, the 2D parameter corresponded to bone mineral density (BMD), quantifying the amount of bone mineral in the tissue by measuring surface bone density per cm^2 in each image (Fig. 3d–g). On the other hand, the bone surface-to-volume ratio (BS/BV) (Fig. 3h–k), is a 3D parameter showing the number of bone lining cells

covering a specific bone volume. μCT analysis showed a significantly decreased BMD in the lateral and medial femoral (0.000845 ± 0.0005080 and 0.001058 ± 0.0006076, respectively) and lateral tibial (0.0007511 ± 0.0005131) joint areas of animals treated with mitochondria at high (1×10^6 M), while by low (0.2×10^6 M) doses it was observed in the medial femoral and lateral tibial (0.0008856 ± 0.0004745 and 0.0006539 ± 0.000444, respectively), as compared to the non-treated group (0.001341 ± 0.0004418, 0.001744 ± 0.0005066 and 0.001301 ± 0.0005718, respectively). Likewise, the BS/BV results showed a reduction at high mitochondria dose-treated animals at lateral-medial tibial and medial femoral (15.77 ± 4.39, 10.83 ± 1.974 and 11.15 ± 1.45, respectively), similarly to the results observed with low mitochondria dose (15.48 ± 3.276, 12.48 ± 2.101 and 12.04 ± 5.145, respectively), concerning non-treated OA mice (22.18 ± 6.824, 18.12 ± 5.853 and 18.35 ± 7.879, respectively). Both parameters confirmed that mitochondria injection displays a beneficial effect in all the areas of the knee, with data approaching the data observed in the sham group. Histological analysis revealed signs of knee joint protection in mice treated with mito-MSC (Fig. 3l–p). The Pritzker OARSI score confirmed the therapeutic potential of mito-MSC. Of note, the beneficial effect of mito-MSC in the four knee joint areas evaluated was more evident when the mice were treated with lower doses than when they were treated with higher doses (Fig. 3m–p). While these results confirm that Mito-MSC transplantation protects cartilage and bone from degradation in the CIOA murine model, they also indicate that a lower dose displays a better beneficial effect.

Mitochondria biodistribution analysis in an experimental model of OA

Biodistribution studies related to local administration in the joint afford invaluable insights regarding the propensity of biologics or pharmacological compounds to accrue within the injection site or to potentially leak to other tissues through the bloodstream. That could engender toxicity effects. To assess the safety of Mito-MSC, we studied the biodistribution profile following intra-articular administration. We performed an intra-articular injection of Mito-MSC at the most effective dose (derived from 200.000 UC-MSC) in OA mice and monitored them over a short time (Fig. 4a). In vivo, scans conducted at 0, 1, 24, 48, and 72 h post-Mito-MSC injection revealed that mitochondria stained with Mitoview™ were not visible after 48 h of IA injection within the detection limit of the equipment used (Fig. 4b). At 72 h post-Mito-MSC mice were euthanized and the lung, heart, and spleen (Supplementary Figure 2) and the nearby popliteal lymph nodes (LN), contralateral LN and inguinal lymph node were obtained (Fig. 4d) No signal was observed after 72 h, suggesting short-term retaining of Mito-MSC on the site of injection, without migration/leakage to neighboring organs (Supplementary Figure 2 and Fig. 4d). Additionally, to assess the potential migration of Mito-MSC, DNA from human mitochondria was assessed in the mouse knee joint and the tissue was analyzed ex vivo. Our results showed that human mitochondrial DNA was detected in all the IA-injected mice right after the injection. However, after 1 and 24 h, human mitochondrial DNA was detected in the joint of half of the total injected mice. Likewise, only one mouse was positive for mitochondrial DNA after IA injection at 48 h and no human DNA was detected at 72 h. Finally, after 48 h, 1 in 4 mice showed a positive signal in nearby LN (Fig. 4e) without any human mitochondrial DNA detection in the contralateral LN nor in the inguinal LN. These findings suggest a favorable safety profile concerning migration to distant organs following IA administration of mitochondria in the OA murine model.

Mitochondria transplantation protects mice from OA inflammatory response

Given that one of the main symptoms of OA patients is the inflammation of the joint and that mitochondrial DNA might generate an immunogenic response [23], we evaluated the immune response induced after Mito-MSC IA injection. To this end, 3 days after IA injection of Mito-MSC (low dose), the mice were euthanized, and the immune response was assessed by measuring the release of pro-inflammatory cytokines and the frequency of inflammatory T cell populations, including T helper (h) 1 and Th17 cells in the nearby popliteal lymph nodes (Fig. 5a). Compared to the OA mice, mice treated with Mito-MSC did not exhibit an increased frequency of CD4 + IFNg + cells (Th1) (Fig. 5b, d). No effect of Mito-MSC treatment was observed on the frequency of pro-inflammatory CD4 + IL17 + (Th17) cells compared with untreated mice (SHAM and OA groups) (Fig. 5e), nor on the generation of anti-inflammatory CD25 + Foxp3 + cells (Treg) (Fig. 5c, g). Overall, these results indicate that Mito-MSC does not induce a pro-inflammatory response in mice with osteoarthritis. Moreover, they also provide a protective effect against chronic inflammation associated with a pro-inflammatory Th1 response.

Discussion

This study represents a comprehensive preclinical investigation aiming to determine the efficacy, dose–response, biodistribution and immunogenicity of mitochondria-derived from UC-MSC (Mito-MSC) in OA and the potential transcriptomic modifications triggered by mitochondria transplantation in a critical OA

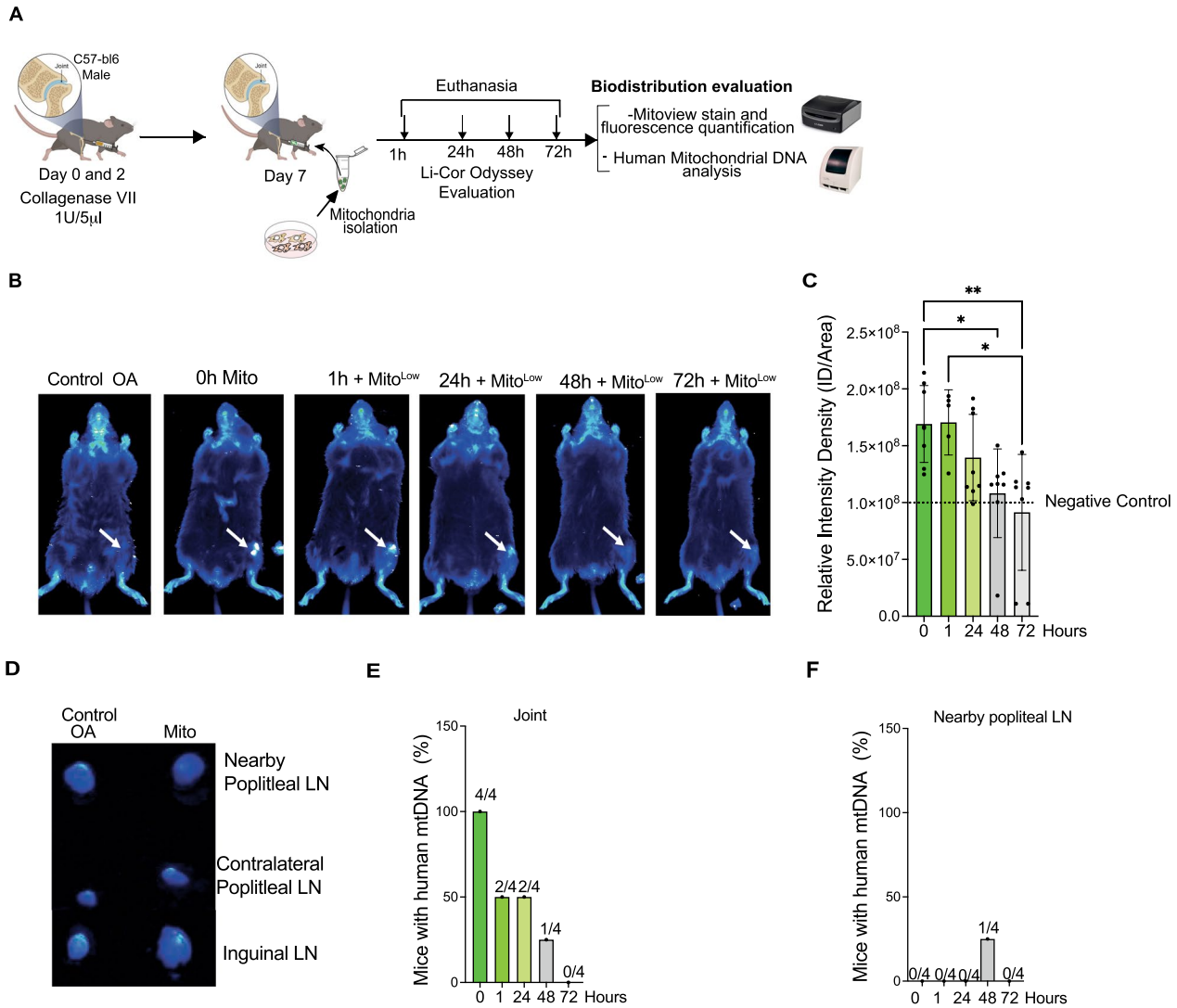

Fig. 4 **a** Biodistribution assay of intraarticular mitochondrial transplantation into the knee in vivo in a murine model of OA. Experimental design of the biodistribution assay of intraarticular mitochondria injection in the CIOA murine model. **b** Representative mice images following intraarticular injections of mitochondria-derived from 200,000 UC-MSC stained with MitoView™ in OA mice (white arrow), evaluated after 0, 1, 24, 48 and 72 h post-treatment by Odyssey CLx Imager. Sodium Chloride (NaCl) was used to control OA mice (left images). **c** Relative fluorescence density quantification of the mitoview intensity in the injected joint evaluated with the FIJI program. **d** Representative nearby popliteal lymph node (LN); Contralateral popliteal LN and drained LN image from mice obtained from mice injected with mitochondria stained with MitoView™ after 72H. Quantification of human Mitochondria DNA (hMT-DNA) in the joint of intraarticular mitochondria injection in OA mice. Quantification of human Mitochondrial DNA (hMT-DNA) in the nearby popliteal LN of intraarticular mitochondria injection in OA mice. Results represent mean ± SD; $*p \leq 0.05$, $**p < 0.01$, $***p < 0.001$. (One-way non-parametric Friedman test) of at least 5 animals per experimental group for 2 independent experiments for luminescence analysis and at least 4 animals per experimental group for hMT-DNA quantification

target cell such as chondrocytes. In recent years, there has been a growing recognition that mitochondrial dysfunction plays a critical role in cartilage degeneration [24], particularly through the production of ROS and inflammation, which can lead to chondrocyte apoptosis [25, 26] and subsequent joint destruction [4]. Consequently, mitochondria transplantation has emerged as a novel approach to address pathologies characterized by impaired mitochondrial function such as OA [27, 28]. Indeed, mitochondrial transplantation from mito-L6 and mito-muscle OA has proven therapeutic effect in a rat OA model [12]. In line with these results, it has been reported that xenogeneic mitochondria transplantation does not induce either an acute or a chronic alloreactivity or an DAMP associated-immunogenic response in an ischemic heart model [29]. However, in the context

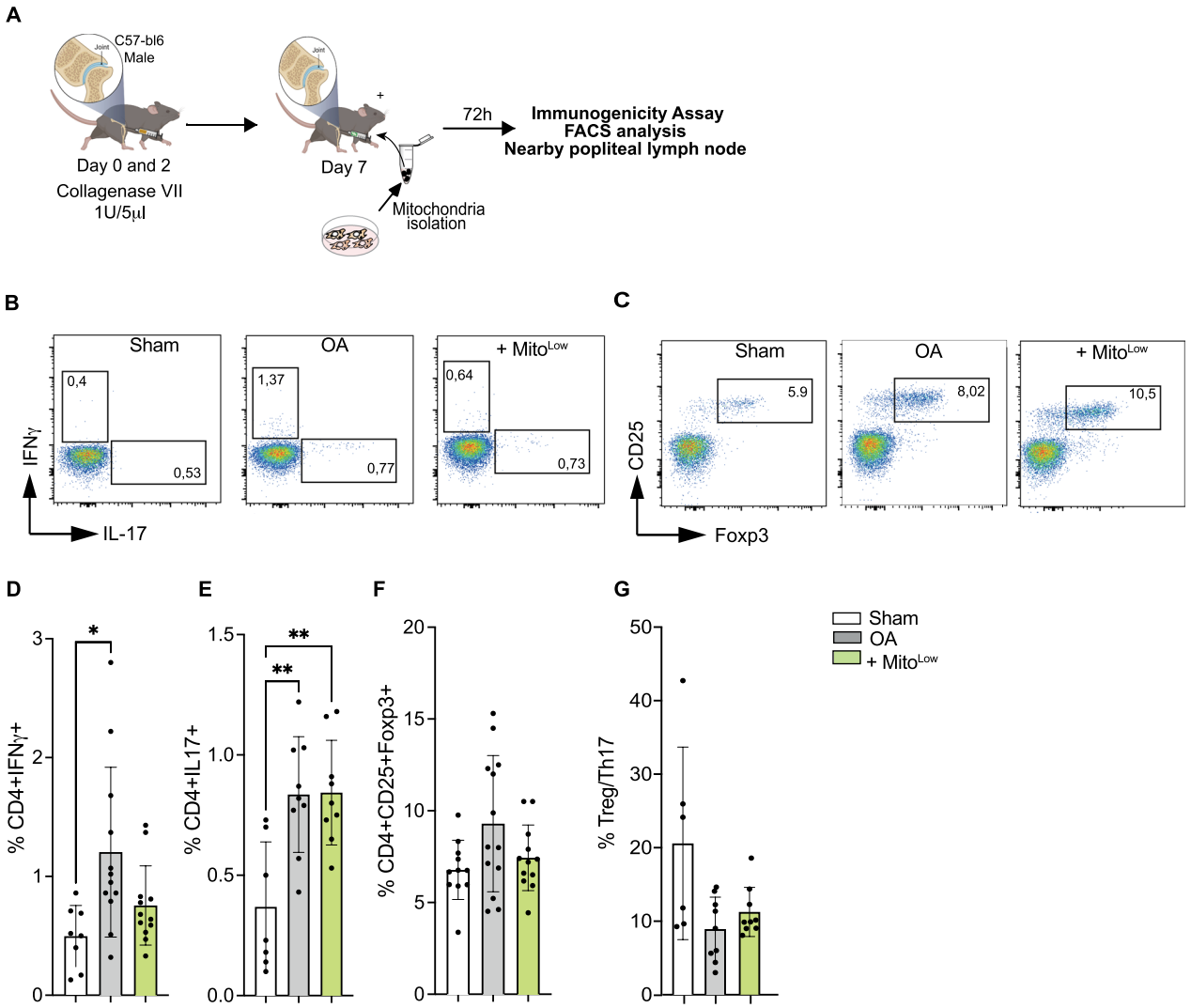

Fig. 5 Immunogenic analysis of mitochondria in the CIOA mice **a** Experimental design of the immunogenic assay of mitochondria in the CIOA murine model. Immune cells were obtained from freshly isolated drained popliteal lymph nodes and were evaluated by FACS analysis. **b** Representative dot plot of FACS images of CD4+ cells positive for IFNγ and IL17 analysis after 72 h of intra articular injections of mitochondria in nearby popliteal LN of OA mice. **c** Representative dot plot images of CD4+ cells positive for CD25 and Foxp3 analysis after 72 h of intraarticular injections of mitochondria in nearby popliteal LN of OA mice. Average quantification in the CD4 positive population of **d** IFNγ positive cells (corresponding to Th1 cells) **e** IL-17 positive cells (corresponding to Th17 cells) **f** CD25 + Foxp3 positive cells (corresponding to Treg cells) **g** Treg/Th17 ratio analysis. Results represent mean ± SD; *$p \leq 0.05$, **$p < 0.01$, ***$p < 0.001$. (One-way ANOVA-test). Experiments were repeated at least 3 times, where for Th17 detection we used at least 6 animals per experimental group on 2 independent experiments and for Th1 and Treg detection experiment was repeated 3 times with at least 9 animals per experimental group

of human therapeutic applications, it is imperative to have a dependable and well-defined source of cells that can be consistently used for clinical purposes. Considering this requirement, MSCs emerge as the preferred candidates for mitochondrial donation, given their demonstrated positive impact on clinical symptoms of OA in phase I clinical studies [13–15]. Therefore, since mitochondrial dysfunction is critical in cartilage degeneration, mitochondria transplantation derived from healthy MSC might represent a better alternative for OA treatment. Indeed, Yu et al. showed that mitochondria and vesicles derived from Bone Marrow MSC exhibit beneficial effects in a rat model of OA [19]. In line with this work, we compare the therapeutic role of UC-MSC and their derived mitochondria and demonstrated that both display beneficial effects in OA progression in a murine model (Currently under review). Here, we show that MSCs can transfer their mitochondria into the main

target cells associated to OA pathogenesis, including chondrocytes, synovial macrophages, and synovial fibroblasts. Consistent with these findings, transcriptomic analysis of chondrocytes indicated differential expression of stress-related genes upon treatment with mitochondria obtained from healthy UC-MSC in OA patients. Our findings corroborate previous research indicating that the transfer of MSC mitochondria to chondrocytes from OA patients increases mitochondrial membrane potential, metabolic activity, and ATP content in chondrocytes, and thus inhibits apoptosis induced by defective mitochondria [20]. This study is consistent with our observations, where we identify changes in stress response gene expression upon Mito-MSC transfer such as Exo1 a gene that encodes the exonuclease 1 that is involved in DNA repair and recombination process [30]. These findings suggest a potential mechanistic pathway for preserving chondrocyte integrity and mitigating degeneration in OA. It has been shown that despite the promising results obtained with MSC in terms of alleviating pain and improving joint functionality in osteoarthritis patients, their beneficial impact on the integrity of cartilage tissue has not been consistently observed [31]. Interestingly, the two doses of Mito-MSC tested in this work significantly protect cartilage from degradation and bone mineral density modifications, a hallmark of OA. However, the lower dose proved more effective in terms of histological score. While other dose ranges can be used to obtain a significant difference, our findings align with observations from a phase I clinical study performed by our group, where it was noted that lower doses of UC-MSC exert a higher beneficial effect as compared to lower doses due to the generation of some adverse effect such as synovitis, where it was observed that high-dose could induce inflammation [13]. It is suggested that the reason a higher dose of mitochondria does not produce the same or better effects as the lower dose is that an excessive addition of mitochondria, beyond what the cells require to revert the dysfunction, may lead to a higher ROS production due to mitochondrial overload, activating inflammatory pathways that counteract the beneficial effects of this cell-free therapy and reducing the therapeutic potential observed at lower doses.

As mentioned before, Lee and Yu et al. previously demonstrated that the intra-articular injection of exogenous mitochondria significantly reduces cartilage destruction in a rat model of OA [12, 19]. However, the authors of both articles did not validate the presence of mitochondria in the joint, neither the permanency, the dose–effect, or the potential immunogenic response. Therefore, we conducted the first biodistribution study that determined the permanency or leakage of the mitochondria administered within the joint space using two different techniques: Fluorescence and Mitochondrial DNA quantification. Our findings reveal that mitochondria remained at the injection site for up to 24 h without leaking into other organs, suggesting that the mitochondria effect (i) is local and probably targeting the main cell components of the knee affected in OA including synovial macrophages, synovial fibroblasts, and chondrocytes and (ii) effective in a short window of time. In contrast, previous studies conducted by authors involved in this research have described that human UC-MSC persists in the joint for up to 7 days, in the same OA in vivo model used here, when injected into the knee joint and are effective on the clinical signs of OA [32]. It is then tempting to speculate that the Mito-MSC and the MSC themselves act via different modes of action and that the mitochondria effect is more immediate because they constitute the effector part of the MSC. This hypothesis remains to be investigated in more detail.

To reinforce the safety assessment, we evaluated the potential immunogenic effect but also the desired anti-inflammatory response triggered by Mito-MSC transplantation. Our results showed that injection of Mito-MSC did not induce any inflammatory response. It appeared to have an inhibitory effect, as evidenced by the suppression of Th1 cells observed in mice after OA induction. As previously indicated, mitochondria are unlikely to induce a pathogenic inflammatory immune response after transplantation into different organs such as the heart [29]. In line with this study, we demonstrated that xenogeneic mitochondria transplantation does not induce an adaptive immunogenic response. Additionally, varying degrees of inflammation can be observed in osteoarthritis [33] and are associated with the severity of the disease. We hypothesize that the injection of Mito-MSC could act powerfully to regulate inflammation, thereby limiting damage to joint tissues and leading to a prevailing beneficial effect in osteoarthritis.

Finally, the transcriptomic analysis showed an increased antiviral immune response prompted by Mito-MSC treated chondrocytes. This result seems to contradict the inhibition of the increase in Th1 frequency induced by the injection of Mito-MSC after the induction of osteoarthritis. We thus propose that this antiviral immune response associated with the activation of the IFNγ molecular pathway might represent a chondroprotective response to inhibit exogenous inflammation. Although this hypothesis requires further investigation, it has previously been reported that chondrocytes can exert immunosuppressive and immunomodulatory effects on immunocompetent cells when activated by pro-inflammatory stimuli such as IFNγ [34], which is consistent with the mitochondria transfer effects findings on this research.

Conclusions

Altogether our data demonstrated that UC-MSC-derived mitochondria injected into the joint of mice serve a protective role against the progression of OA probably through the induction of protective transcriptional changes on target cells such as chondrocytes. Moreover, is the first study to demonstrate their permanency within the joint over time for up to 24 h, exhibiting non-inflammatory characteristics. These findings introduce a safe cell-free acellular therapy based on mitochondria derived from MSC as an innovative therapeutic approach for OA treatment.

Supplementary Information

The online version contains supplementary material available at https://doi.org/10.1186/s12967-024-05945-7.

Additional file 1.

Additional file 2. Figure S1. MicroCT trabecula thickness analysis of the CIOA murine model. Average quantification of thickness (cm^2) for A) Medial Tibia. B) Lateral Tibia. C) Lateral femur and D) Medial femur. Results represent mean ± SD; $*p \leq 0.05$, $**p < 0.01$, $***p < 0.001$. (One-way ANOVA test) of N = 16 for 2 independent experiments.

Additional file 3. Figure S2. Representative organ imaging obtained from OA-mice injected or not with mitochondria stained with mitoview after 72H. From upper organs: Lung, Heart and Spleen

Acknowledgements

We thank Javiera Ponce for their veterinary assistance on the Animal facilities of C4C and the clinical staff of the Clinica Universidad de los Andes and Hospital Clinico Universidad de Chile.

Author contributions

PLC, AMV and CG perform the experimental design with inputs from FF, FD and MK. AMV and CG perform the biodistribution, immunogenicity and efficacy experiments and the microCT and FACS analysis with inputs from RV, DP, AC and YH. LYF, MB, JM, NJ, RL, GA, ADC, JT, CP, CAV, NLC, MJA, FV and FT perform the in vitro experiments and analysis. LYF performs biodistribution quantification. ELB, CP, YH, LC, YH and AC participate in the biodistribution analysis by human mitochondria DNA detection in vivo. AO, JB and FB participate in the histological preparation and analysis. REV, MR, CC, KO, CF perform the Affymetrix analysis. PLC, AMV, REV and CG wrote the manuscript with inputs from MK, FF, FD, ADC, KO and AC.

Funding

This work was supported by ANID-Fondecyt Regular PLC No. 1211353; Fondecyt Iniciación AMV No. 11220549; Fondecyt Regular FF, Fondecyt Postdoctoral FB 3220204; Fondecyt Regular No. 1211749 MK; Fondecyt Regular 1230428 ADC; and Fondecyt Iniciación 11221017 YHF. ANID-Basal funding for Scientific and Technological Center of Excellence, IMPACT, Interventional Medicine for Precision and Advanced Cellular Therapy, #FB210024 and FONDEF ID21I10194 PLC and CF was supported by ANID SIA/PAI code SA77210106. This work was also supported by the "Programme Inserm International Research Project" (PRI-MitoMir project) and by the "Agence nationale de la recherche" (ANR) with the project METAB-OA (ANR-20-CE18-0014).

Availability of data and materials

The datasets supporting the conclusions of this article are available on Zenodo record 14172161: https://zenodo.org/records/14172161. Further material inquiries can be addressed to the corresponding author.

Declarations

Consent for publication

All authors give their consent for publication.

Competing interests

Dr. Maroun Khoury is the chief scientific officer of Cells for Cells, EVast Bio (both are Spin-off from the Universidad de los Andes, Chile), and REGENERO a Chilean consortium for regenerative medicine. He reports receiving grants from ANID (National agency for research and development) and stipend from Cells for Cells under a research contract with the Universidad de los Andes, Chile. In addition, Dr. Khoury is the inventor of patents related to mesenchymal stem cells including a patent WO2014135924A1 pending, a patent WO2017064670A2 pending, a patent WO2017064672A1 pending, and a patent WO/2019/051623 pending. Andrés Caicedo is the scientific founder and advisor of Dragon Biomed, an entrepreneurial initiative at the Universidad San Francisco de Quito (USFQ). He also serves as a scientific advisor in the Research and Development department of Luvigix. In these roles, he provides scientific guidance and expertise but does not participate in the decision-making processes or operational activities of either company.

Author details

[1]Center of Interventional Medicine for Precision and Advanced Cellular Therapy, IMPACT, Santiago, Chile. [2]Centro de Investigación e Innovación Biomédica, Facultad de Medicina, Universidad de Los Andes, Santiago, Chile. [3]Cells for Cells and Regenero the Chilean Consortium for Regenerative Medicine, Santiago, Chile. [4]IRMB, Université de Montpellier, INSERM, Montpellier, France. [5]Facultad de Odontología, Universidad de Chile, Santiago, Chile. [6]Departamento de Ciencias Veterinarias y Salud Pública, Facultad de Recursos Naturales, Universidad Católica de Temuco, Temuco, Chile. [7]Laboratorio de Biología Celular, Departamento de Biología Celular, Facultad de Ciencias Biológicas, Universidad de Concepción, Concepción, Chile. [8]Red de Equipamiento Científico Avanzado-REDECA, Facultad de Medicina, Universidad de Chile, Santiago, Chile. [9]Escuela de Ingeniería Bioquímica, Pontificia Universidad Católica de Valparaíso, Valparaíso, Chile. [10]Laboratorio de Neuroinmunología, Facultad de Medicina y Ciencia, Universidad San Sebastián, Sede Concepción, Chile. [11]Laboratorio de Fisiología y Bioenergetica Celular, Pontificia Universidad Católica de Chile, Santiago, Chile. [12]Laboratorio de Investigación en Ciencias Biomédicas, Departamento de Ciencias Básicas y Morfología, Facultad de Medicina, Universidad Católica de la Santísima Concepción, Concepción, Chile. [13]Universidad San Francisco de Quito USFQ, Colegio de Ciencias de la Salud e Instituto de Investigaciones en Biomedicina iBioMed, Escuela de Medicina, Quito, Ecuador-Mito-Act Research Consortium, Quito, Ecuador. [14]CHU Montpellier, Montpellier, France. [15]Departamento de Ortopedia y Traumatología, Hospital Clinico Universidad de Chile, Independencia, Chile.

Received: 10 June 2024 Accepted: 5 December 2024
Published online: 07 January 2025

References

1. Han S. Osteoarthritis year in review 2022: Biology. Osteoarthritis Cartilage. 2022.
2. Bijlsma JW, Berenbaum F, Lafeber FP. Osteoarthritis: an update with relevance for clinical practice. Lancet. 2011;377(9783):2115–26.
3. Yao Q, Wu X, Tao C, Gong W, Chen M, Qu M, et al. Osteoarthritis: pathogenic signaling pathways and therapeutic targets. Signal Transduct Target Ther. 2023;8(1):56.
4. Reed KN, Wilson G, Pearsall A, Grishko VI. The role of mitochondrial reactive oxygen species in cartilage matrix destruction. Mol Cell Biochem. 2014;397(1–2):195–201.
5. Qi Z, Zhu J, Cai W, Lou C, Li Z. The role and intervention of mitochondrial metabolism in osteoarthritis. Mol Cell Biochem. 2023.
6. Shen P, Serve S, Wu P, Liu X, Dai Y, Durán-Hernández N, et al. NOS inhibition reverses TLR2-induced chondrocyte dysfunction and attenuates age-related osteoarthritis. Proc Natl Acad Sci U S A. 2023;120(29):e2207993120.

7. Emani SM, Piekarski BL, Harrild D, Del Nido PJ, McCully JD. Autologous mitochondrial transplantation for dysfunction after ischemia-reperfusion injury. J Thorac Cardiovasc Surg. 2017;154(1):286–9.
8. McCully JD, Cowan DB, Pacak CA, Toumpoulis IK, Dayalan H, Levitsky S. Injection of isolated mitochondria during early reperfusion for cardioprotection. Am J Physiol Heart Circ Physiol. 2009;296(1):H94–105.
9. Luque-Campos N RR, Molina L, Canedo-Marroquin G, Vega-Letter AM, Luz-Crawford P, Bustamante-Barrientos FA. Exploring the therapeutic potential of the mitochondrial transfer-associated enzymatic machinery in brain degeneration. Frontiers in Physiology Sec Mitochondrial Research. 2023;14.
10. Bustamante-Barrientos FA, Luque-Campos N, Araya MJ, Lara-Barba E, de Solminihac J, Pradenas C, et al. Mitochondrial dysfunction in neurodegenerative disorders: potential therapeutic application of mitochondrial transfer to central nervous system-residing cells. J Transl Med. 2023;21(1):613.
11. Borcherding N, Brestoff JR. The power and potential of mitochondria transfer. Nature. 2023;623(7986):283–91.
12. Lee AR, Woo JS, Lee SY, Na HS, Cho KH, Lee YS, et al. Mitochondrial transplantation ameliorates the development and progression of osteoarthritis. Immune Netw. 2022;22(2): e14.
13. Matas J, García C, Poblete D, Vernal R, Ortloff A, Luque-Campos N, et al. A phase I dose-escalation clinical trial to assess the safety and efficacy of umbilical cord-derived mesenchymal stromal cells in knee osteoarthritis. Stem Cells Transl Med. 2024.
14. Pers YM, Rackwitz L, Ferreira R, Pullig O, Delfour C, Barry F, et al. Adipose mesenchymal stromal cell-based therapy for severe osteoarthritis of the knee: a phase i dose-escalation trial. Stem Cells Transl Med. 2016;5(7):847–56.
15. Gupta PK, Chullikana A, Rengasamy M, Shetty N, Pandey V, Agarwal V, et al. Efficacy and safety of adult human bone marrow-derived, cultured, pooled, allogeneic mesenchymal stromal cells (Stempeucel®): preclinical and clinical trial in osteoarthritis of the knee joint. Arthritis Res Ther. 2016;18(1):301.
16. Tejedor G, Luz-Crawford P, Barthelaix A, Toupet K, Roudières S, Autelitano F, et al. MANF produced by MRL mouse-derived mesenchymal stem cells is pro-regenerative and protects from osteoarthritis. Front Cell Dev Biol. 2021;9: 579951.
17. Maumus M, Manferdini C, Toupet K, Chuchana P, Casteilla L, Gachet M, et al. Thrombospondin-1 partly mediates the cartilage protective effect of adipose-derived mesenchymal stem cells in osteoarthritis. Front Immunol. 2017;8:1638.
18. Korpershoek JV, Rikkers M, Wallis FSA, Dijkstra K, Te Raa M, de Knijff P, et al. Mitochondrial transport from mesenchymal stromal cells to chondrocytes increases DNA content and proteoglycan deposition. Cartilage. 2022;13(4):133–47.
19. Yu M, Wang D, Chen X, Zhong D, Luo J. BMSCs-derived mitochondria improve osteoarthritis by ameliorating mitochondrial dysfunction and promoting mitochondrial biogenesis in chondrocytes. Stem Cell Rev Rep. 2022;18(8):3092–111.
20. Fahey M, Bennett M, Thomas M, Montney K, Vivancos-Koopman I, Pugliese B, et al. Mesenchymal stromal cells donate mitochondria to articular chondrocytes exposed to mitochondrial, environmental, and mechanical stress. Sci Rep. 2022;12(1):21525.
21. Caicedo A, Fritz V, Brondello JM, Ayala M, Dennemont I, Abdellaoui N, et al. MitoCeption is a new tool to assess the effects of mesenchymal stem/stromal cell mitochondria on cancer cell metabolism and function. Sci Rep. 2015;5:9073.
22. Pritzker KP, Gay S, Jimenez SA, Ostergaard K, Pelletier JP, Revell PA, et al. Osteoarthritis cartilage histopathology: grading and staging. Osteoarthr Cartil. 2006;14(1):13–29.
23. Hu MM, Shu HB. Mitochondrial DNA-triggered innate immune response: mechanisms and diseases. Cell Mol Immunol. 2023;20(12):1403–12.
24. Blanco FJ, Rego I, Ruiz-Romero C. The role of mitochondria in osteoarthritis. Nat Rev Rheumatol. 2011;7(3):161–9.
25. Li D, Xie G, Wang W. Reactive oxygen species: the 2-edged sword of osteoarthritis. Am J Med Sci. 2012;344(6):486–90.
26. Xiao SQ, Cheng M, Wang L, Cao J, Fang L, Zhou XP, et al. The role of apoptosis in the pathogenesis of osteoarthritis. Int Orthop. 2023;47(8):1895–919.
27. Ahmad T, Mukherjee S, Pattnaik B, Kumar M, Singh S, Rehman R, et al. Miro1 regulates intercellular mitochondrial transport & enhances mesenchymal stem cell rescue efficacy. EMBO J. 2014;33(9):994–1010.
28. Court AC, Vega-Letter AM, Parra-Crisóstomo E, Velarde F, García C, Ortloff A, et al. Mitochondrial transfer balances cell redox, energy and metabolic homeostasis in the osteoarthritic chondrocyte preserving cartilage integrity. Theranostics. 2024;14(17):6471–86.
29. Ramirez-Barbieri G, Moskowitzova K, Shin B, Blitzer D, Orfany A, Guariento A, et al. Alloreactivity and allorecognition of syngeneic and allogeneic mitochondria. Mitochondrion. 2019;46:103–15.
30. Lemaçon D, Jackson J, Quinet A, Brickner JR, Li S, Yazinski S, et al. MRE11 and EXO1 nucleases degrade reversed forks and elicit MUS81-dependent fork rescue in BRCA2-deficient cells. Nat Commun. 2017;8(1):860.
31. Matas J, Orrego M, Amenabar D, Infante C, Tapia-Limonchi R, Cadiz MI, et al. Umbilical cord-derived mesenchymal stromal cells (MSCs) for knee osteoarthritis: repeated MSC dosing is superior to a single MSC dose and to hyaluronic acid in a controlled randomized phase I/II trial. Stem Cells Transl Med. 2019;8(3):215–24.
32. Matas J, García C, Poblete D, Vernal R, Ortloff A, Luque-Campos N, et al. A phase I dose-escalation clinical trial to assess the safety and efficacy of umbilical cord-derived mesenchymal stromal cells in knee osteoarthritis. Stem Cells Transl Med. 2024;13(3):193–203.
33. Motta F, Barone E, Sica A, Selmi C. Inflammaging and osteoarthritis. Clin Rev Allergy Immunol. 2023;64(2):222–38.
34. Osiecka-Iwan A, Hyc A, Radomska-Lesniewska DM, Rymarczyk A, Skopinski P. Antigenic and immunogenic properties of chondrocytes. Implications for chondrocyte therapeutic transplantation and pathogenesis of inflammatory and degenerative joint diseases. Cent Eur J Immunol. 2018;43(2):209–19.

Publisher's Note